Ikeda Hopf bifurcation revisited

T. Erneux, L. Larger, Min Won Lee, Jean-Pierre Goedgebuer

Ikeda Hopf bifurcation revisited

Thomas Erneux [a,*], Laurent Larger [b,c], Min Won Lee [b,c], Jean-Pierre Goedgebuer [b,c]

[a] *Université Libre de Bruxelles, Optique Nonlinéaire Théorique, Campus Plaine, C. P. 231, 1050 Bruxelles, Belgium*
[b] *GTL-CNRS Telecom, UMR 6603, 2–3 rue Marconi, 57070 Metz, France*
[c] *Laboratoire d'Optique P. M. Duffieux, UMR 6603 CNRS, Université de Franche-Comté, Route de Gray, 25030 Besançon Cedex, France*

Abstract

A large variety of passive optical systems subject to a delayed feedback have appeared in the literature and are described mathematically by the same class of scalar delay differential equations (DDEs). These equations include Ikeda DDE and their solutions are determined in terms of a control parameter distinct from the delay. We concentrate on the first Hopf bifurcation generated by a fixed delay and determine a general expression for its direction of bifurcation. We then examine our result in the two limits of small and large delays. For small delays, we show that a Hopf bifurcation to nearly sinusoidal oscillations is possible provided that the feedback rate is sufficiently high (bifurcation from infinity). For large delays, we complement the early work by Chow et al. [Proc. Roy. Soc. Edinburgh A 120 (1992) 223–229] and Hale and Huang [J. Diff. Equ. 114 (1994) 1–23] by comparing analytical and numerical bifurcation diagrams as the oscillations progressively change from sine to square-wave.

Keywords: Hopf bifurcation; Delay difference equations; Nonlinear optics

1. Introduction

In 1979, Kensuke Ikeda considered a nonlinear absorbing medium containing two-level atoms placed in a ring cavity and subject to a constant input of light (see Fig. 1). If the total length of the cavity is sufficiently large, the optical system undergoes a time-delayed feedback which destabilizes its steady state output. From the Maxwell–Bloch equations, Ikeda derived a set of delay differential equations [23]. This derivation is simpler if we start from the Maxwell–Debye equations for highly dispersive media [24]. These equations are given by the following coupled differential difference equations (see [37, p. 122]; [40, p. 39]):

$$E = A + BE(t - t_D)\exp(\mathrm{i}(\phi - \phi_0)), \tag{1}$$

$$\tau\phi' = -\phi + |E(t - t_D)|^2, \tag{2}$$

* Corresponding author. Tel. : +32-2-650-5819; fax: +32-2-650-5824.
E-mail address: terneux@ulb. ac. be (T. Erneux).

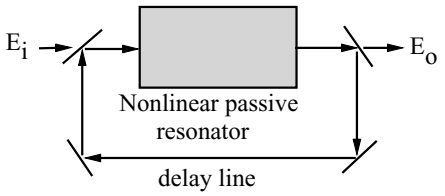

Fig. 1. Ikeda considered the case of a nonlinear passive cavity located in a ring resonator and modeled by a delay differential equation (DDE). E_{i} and E_{o} are the amplitudes of the injected and output fields, respectively. The delay is the round-trip time along the optical-path.

where E is the field at the boundary of the ring cavity where input and feedback lights are combined. ϕ is the phase shift experienced by the electrical field in the medium and ϕ_0 is the linear phase shift across the medium. The parameter A is proportional to the incident light intensity. The parameter B characterizes the dissipation of the electrical field in the cavity. The quadratic coefficient of the nonlinear refractive index is assumed positive implying a positive coefficient for $|E(t-t_D)|^2$ in Eq. (2). τ is the Debye relaxation time and t_D is the propagation time of the light in the ring cavity. Assuming strong dissipation (small B), high input intensity (large A) but keeping A^2B fixed, Eqs. (1) and (2) can be reduced to the following scalar DDE [24,33]:

$$\tau\phi' = -\phi + A^2[1 + 2B\,\cos\,(\phi(t-t_D) - \phi_0)], \tag{3}$$

which is known as Ikeda DDE. Ikeda then showed numerically that periodic and chaotic outputs are possible. In 1983, the experimental system has been realized by his colleagues with a train of light pulses injected in a long single mode optical fibre [25] but the Ikeda physical system is poorly described by Eq. (3). Efforts to develop an experimental device that is accurately modeled by a simple DDE like Eq. (3) immediately followed the early work of Ikeda. We briefly review these studies and emphasize quantitative comparisons between experiments and theory.

From the basic idea of Ikeda, an optical system has been realized by Gibbs et al. [15] in 1981. Their system is based on a bistable opto-electronical system with delay and its behavior can be described by Eq. (3). An improved device is studied in [22] and is modeled mathematically by

$$\tau X' = -X + \pi\mu[1 - \,\sin\,(X(t-t_D))]. \tag{4}$$

Here X is proportional to the voltage fed to a potassium dehydrogen phosphate (KDP) modulator. μ is proportional to the input intensity and is our control parameter. The output signal is injected into a photodiode and delayed using a computer. The delay $t_D = 36\,\mathrm{ms}$ is much larger than $\tau = 0.8\,\mathrm{ms}$. Several bifurcation phenomena were observed including chaos and demonstrate experimentally Ikeda's early predictions. If $\tau/t_D \ll 1$, we may neglect the X' term and consider the equation for a map relating $X(t_{n+1})$ and $X(t_n)$ ($t_n = nt_R$): $X_{n+1} = \pi\mu[1 - \,\sin\,(X_n)]$. The map is an important simplification of the bifurcation problem and its validity to describe the Hopf bifurcation will be addressed in this paper. How well Eq. (4) predicts the output of the experiment is discussed in [22].

Another experimental system was realized by Neyer and Voges [38] in 1982. It is the first experimental system which used an integrated optical component. This system is based on the use of an electro-optical Mach–Zehnder (MZ) modulator. The response of the system was described by a map $u_{n+1} = F(u_n, G)$, where u is the applied voltage and G is proportional to the input intensity. The relatively large delay of $1\,\mu\mathrm{s}$ is obtained using a $200\,\mathrm{m}$ coaxial cable.

An acousto-optical system has also been studied in Quebec by Vallée and Delisle [43]. This system is described by the DDE

$$\tau X' + X = \pi(A - \lambda\,\sin^2(X(t-t_D) + X_B)), \tag{5}$$

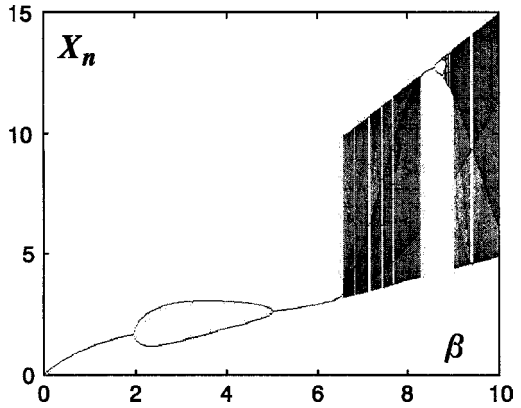

Fig. 2. Bifurcation diagram of the fixed points $X_n = X_n(\beta)$.

where λ is the control parameter, $A = 0.5$ is an offset of X, and $X_B = \pi/4$ is a phase shift. The 2 km of optical fibre produced a delay $t_D = 10\,\mu$s. The responses obtained with different delays $t_D/\tau = 0.84, 2.6, 16$ demonstrated experimentally the importance of the delay.

In France, work has been done on an delayed optical system where the dynamical variable is the wavelength [9,16]. An improved device using a tunable DBR laser was then realized [17,28]. This experience then led to the development of a system based on coherence modulation [31]. The dynamical variable is the optical-path difference in a coherent modulator driven electrically by a nonlinear delayed feedback loop [29]. The system is realized from a MZ coherence modulator powered by a short coherence source and driven by a nonlinear feedback loop that contains a second MZ interferometer and a delay line. In dimensionless variables, the response of the system is well described by [31]

$$\tau X' = -X + \beta[1 + \tfrac{1}{2}\cos(X(t - t_D) + \Phi)], \tag{6}$$

where X is proportional to the optical-path difference. The bifurcation parameter β is proportional to the photodetector gain K which can be varied. The phase Φ can be changed electrically by means of a bias voltage applied to the first MZ. Experimentally, the ratio t_D/τ is chosen sufficiently large so that the equation for the map is a valid approximation. It is given by

$$X_{n+1} = \beta[1 + \tfrac{1}{2}\cos(X_n + \Phi)]. \tag{7}$$

The bifurcation diagram of the fixed points of Eq. (7) is shown in Fig. 2 for $\Phi = 0$ [31]. They have been determined after all transient points disappeared. Numerical and experimental values of the first three bifurcations are compared in the next table and show quantitative agreement.

	$\Phi = 0$		
Numerical	2. 08	5. 04	6. 59
Experimental	2. 07	5. 30	6. 69

The first two bifurcations are Hopf bifurcations while the third bifurcation marks a sudden transition to chaotic dynamics.

All the optical systems that we have reviewed are described by the same class of scalar DDEs given by

$$\varepsilon y' = -y + f(\lambda, y(t - 1)). \tag{8}$$

Here y' denotes the derivative of y with respect to the dimensionless time t ($t \equiv t'/t_d$, where t_d is the delay time). The fixed parameter $\varepsilon \equiv \tau/t_d$ is defined as the ratio between the linear decay time of the dependent variable and the delay time. In Eq. (8), $f(\lambda, y)$ represents a nonlinear function of y and λ is a control parameter. Closely related to the DDE (8) is the equation obtained by setting $\varepsilon = 0$ in (8) and given by

$$-y + f(\lambda, y(t-1)) = 0. \tag{9}$$

Eq. (9) is the equation for a map generating $y_n \equiv y(t)$ as a function of $y_{n-1} \equiv y(t-1)$ of the form

$$y_n = f(\lambda, y_{n-1}). \tag{10}$$

The DDE (8) is called a delay recruitment equation [11] in the context of biological or medical applications. Note that Eq. (8) exhibits a simple damping term $(-y)$ and that the nonlinear function f only depends on $y(t-1)$. DDEs such as the linear growth or decay equation, $\varepsilon y' = \pm y(t-1)$ [8], and the delayed logistic equation, $\varepsilon y' = \lambda y(1-y(t-\tau))$ [12], do not belong to this class of equations. Eq. (8) with specific nonlinear functions have been studied. Mackey [32] studied the case of an autoimmune disease that causes periodic crashes in the production of red blood cells. He formulated an equation exhibiting a delayed negative feedback which can be rewritten as

$$\varepsilon\lambda y' = -y + \lambda[1 + y^p(t-1)]^{-1}. \tag{11}$$

Eq. (11) is almost of the form (8) except that the bifurcation parameter appears both in the nonlinear function and in the left hand side. Schanz and Pelster [42] studied the synchronization of two coupled oscillators and investigated Eq. (8) with $f(\lambda, y) = -\lambda \sin(y)$, where $\lambda > 0$. Hong et al. [21] examined the bifurcation diagram of Eq. (8) with $f(\lambda, y) = 1 - \lambda y^2$. Finally one Ikeda equation where

$$f(\lambda, y) = \lambda(1 - \sin(y)), \tag{12}$$

has been investigated in detail for its period doubling bifurcations [34,35].

A systematic analysis of the direction of bifurcation for the Hopf bifurcation in terms of an arbitrary function f has been developed by Giannakopoulos and Zapp [13,14]. The authors used center manifold techniques and considered the delay as the bifurcation parameter. The delay is a convenient parameter for mathematical analysis but not for our optical devices where the delay is fixed and a different parameter is used as the control parameter. Moreover, we are interested to analyze how the Hopf bifurcation changes in the two limits of large or small delays. A general formula for the direction of bifurcation is also derived by Diekmann et al. [6] by the center manifold. In this paper, we investigate the Hopf bifurcation problem using λ as an arbitrary bifurcation parameter. We use the Lindstedt–Poincaré method [7,26,36] to determine a small amplitude periodic solution and then investigate its validity for small or large delays (large or small values of ε, respectively). In addition to the direction of bifurcation, we analyze the correction of the frequency and the correction of the leading approximation of the solution. These corrections reveal how the regular Hopf expansion of the solution becomes nonuniform for small or large ε and suggest new expansions of the solution.

The paper is organized as follows. In Section 2, we briefly describe how the stability properties of the steady state solutions can be determined analytically from Eq. (8). In Section 3, we summarize the results of a bifurcation analysis near the first Hopf bifurcation point. In Section 4, we use the method of matched asymptotic expansions [3,27] and investigate how the nearly harmonic oscillations near the Hopf bifurcation point progressively change into square-wave.

2. Steady state and Hopf bifurcation

In this section, we determine the steady state solutions and analyze the Hopf bifurcation conditions. This analysis is more frequently done for the map (10) [33] but, as we shall demonstrate, it is instructive to analyze the DDE (8).

2.1. Steady and Hopf bifurcation points

The steady state solution $y_s(\lambda)$ satisfies the equation

$$-y_s + f(\lambda, y_s) = 0. \tag{13}$$

In order to study its stability, we formulate the linearized equation for a small perturbation $u = y - y_s$. This equation is given by

$$\varepsilon u' = -u + f_y(\lambda, y_s)u(s-1), \tag{14}$$

where $f_y(\lambda, y_s)$ represents a partial derivative of the function f evaluated at $y = y_s(\lambda)$.

We first seek a solution of Eq. (14) of the form $u = c\exp(\sigma s)$, where σ is real. From Eq. (14), we then obtain an implicit solution for $\sigma = \sigma(f_y)$. We find that $\sigma > 0$ ($\sigma < 0$) if

$$f_y(\lambda, y_s) > 1 \quad (f_y(\lambda, y_s) < 1). \tag{15}$$

The critical point defined by the condition

$$f_y(\lambda, y_s) = 1 \tag{16}$$

is a steady bifurcation point which is characterized by one single zero eigenvalue.

We next seek a solution of the form $u = c\exp(\sigma s)$, where $\sigma = \sigma_r + i\sigma_i$ is complex. From (14), we find two conditions for σ_r and σ_i. Eliminating $f_y \exp(-\sigma_r)$, we obtain

$$\sigma_r = -\varepsilon^{-1} - \frac{\sigma_i}{\tan(\sigma_i)}, \tag{17}$$

and eliminating the trigonometric functions, we obtain

$$f_y(\lambda, y_s) = \pm\sqrt{\exp(2\sigma_r)[(1+\varepsilon\sigma_r)^2 + \varepsilon^2\sigma_i^2]}, \tag{18}$$

where $f_y > 0$ ($f_y < 0$) if $\cos(\sigma_i) > 0$ ($\cos(\sigma_i) < 0$). The solution is in parametric form; we first determine $\sigma_r = \sigma_r(\sigma_i)$ from Eq. (17) and then $f_y = f_y(\sigma_i)$ from Eq. (18).

The Hopf bifurcation point $(y, \lambda) = (y_c, \lambda_c)$ satisfies the conditions $\sigma_i = \omega$ and $\sigma_r = 0$. From (17) and (18), we obtain

$$\tan(\omega) = -\varepsilon\omega, \tag{19}$$

$$f_y(\lambda_c, y_c) = \pm\sqrt{1+\varepsilon^2\omega^2}, \tag{20}$$

where $f_y > 0$ ($f_y < 0$) if $\cos(\omega) > 0$ ($\cos(\omega) < 0$). Note from (20) that the $f_y > 0$ Hopf bifurcation point satisfies the inequality $f_y > 1$. But because of (15), this Hopf bifurcation is already unstable. In the rest of the paper, we mainly concentrate on the $f_y < 0$ Hopf bifurcation. For large delay ($\varepsilon \to 0$), we find $\omega = \pi$ and $f_y = \pm 1$ and together with the steady state condition (13), we may determine the limiting solutions for λ_c and y_c which are O(1) quantities. For small delays ($\varepsilon \to \infty$), we find $\omega = \pi/2$ and $f_y = \pm\varepsilon\pi/2$. This large value of f_y might not be possible for every $f(\lambda, y)$. From (13), we find that the slope of the steady state branch is $\mathrm{d}y_s/\mathrm{d}\lambda = f_\lambda(1-f_y)^{-1}$. It

indicates that a large $|f_y|$ implies $\mathrm{d}y_s/\mathrm{d}\lambda = \mathrm{O}(\varepsilon^{-1})$ small, i. e., a small change of y_s as λ is changed. This is possible for Ikeda function (12). In this paper, we discuss the Hopf bifurcation for large delays in terms of a general function f and then for Ikeda function (12) while we restrict our analysis to Ikeda function in the case of small delays.

2.2. Ikeda small delay

Using (12), the steady state Eq. (13) leads to the implicit solution

$$\lambda = \frac{y_s}{1 - \sin(y_s)}. \tag{21}$$

Since $f_y = -\lambda_c \cos(y_c)$, the two Hopf bifurcation conditions (19) and (20) for $(y, \lambda) = (y_c, \lambda_c)$ are

$$\tan(\omega) = -\varepsilon\omega, \tag{22}$$

$$\lambda_c \cos(y_c) = \mp\sqrt{1 + \varepsilon^2\omega^2}. \tag{23}$$

These conditions must be solved together with Eq. (21) evaluated at $(y_s, \lambda) = (y_c, \lambda_c)$. Using (21), we may eliminate λ_c in Eq. (23) and obtain an equation for y_c only which is given by

$$y_c \cos(y_c) = \mp(1 - \sin(y_c))\sqrt{1 + \varepsilon^2\omega^2}. \tag{24}$$

Thus, we solve Eq. (22) for $\omega(\varepsilon)$, determine $y_c(\varepsilon)$ from (24), and $\lambda_c(\varepsilon)$ from (21) with $y_s = y_c$. For small delays ($\varepsilon \to \infty$), we find from Eq. (22) that the first Hopf bifurcation exhibits the frequency

$$\omega(\infty) = \tfrac{1}{2}\pi. \tag{25}$$

From (24) and (21), we then obtain a solution satisfying $0 < y_c < \pi/2$ given by

$$y_c \simeq \frac{\pi}{2} - \frac{2}{\varepsilon} \quad \text{and} \quad \lambda_c \simeq \frac{\pi}{4}\varepsilon^2. \tag{26}$$

The expression (26) shows that a Hopf bifurcation is always possible even if the delay is small. As the delay increases from zero, the Hopf bifurcation point emerges from infinity ($\lambda_c = \mathrm{O}(\varepsilon^2) \to \infty$ as $\varepsilon \to \infty$) and is called a bifurcation from infinity [41]. A nonlinear analysis that takes into account the scaling properties shown in (26) is possible and leads to a DDE with a quadratic nonlinearity [10].

2.3. Ikeda large delay

For large delays ($\varepsilon \to 0$), we find from Eq. (22) that the first Hopf bifurcation exhibits the frequency

$$\omega_0 \equiv \omega(0) = \pi, \tag{27}$$

and that $y_0 \equiv y_c(0)$ satisfies the transcendental equation

$$y_0 \cos(y_0) - 1 + \sin(y_0) = 0 \quad (f_y = -1) \tag{28}$$

or

$$-y_0 \cos(y_0) - 1 + \sin(y_0) = 0 \quad (f_y = 1). \tag{29}$$

In the latter case, the Hopf bifurcation point exactly coalesces with the steady bifurcation point satisfying (16). This Hopf bifurcation is clearly degenerate since it corresponds to a double zero eigenvalue [18]. See Fig. 3 . Table 1 gives the three first Hopf bifurcation points shown in Fig. 3 and satisfying either Eq. (28) or (29).

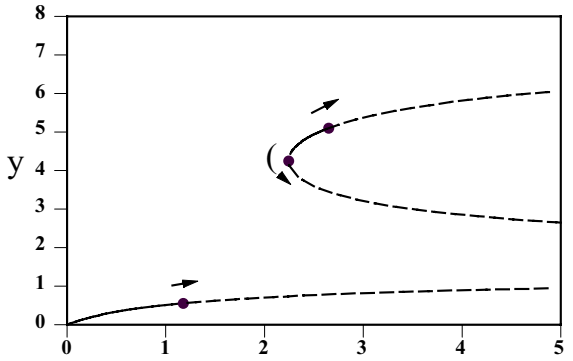

Fig. 3. Bifurcation diagram. Three Hopf bifurcation points as $\varepsilon = 0$ are shown. The arrows indicate how they move as ε increases from zero. Full and dotted lines indicate stable and unstable steady states, respectively.

Table 1
Location of the Hopf bifurcations (only the first and third Hopf bifurcation points may lead to stable oscillations)

	λ_0	y_0	
$f_y = -1$	1. 18	0. 56	Hopf
$f_y = 1$	2. 24	4. 25	Saddle-Hopf
$f_y = -1$	2. 65	5. 10	Hopf

Fig. 4 represents the first Hopf bifurcation point in parameter space (λ, ε). It has been obtained numerically from Eq. (22), (21) and (24). The curve starts at $\lambda = 1.18$ and approaches the large ε parabolic limit given in (26). A better numerical approximation for is given by the parametric solution

$$\varepsilon = -\frac{\tan(\omega)}{\omega}, \tag{30}$$

$$\lambda \simeq \frac{1}{\pi}\sqrt{1 + \tan^2(\omega)}[2 + \sqrt{1 + \tan^2(\omega)}], \tag{31}$$

which is obtained from Eq. (22), (21) and (24) for ε large by expanding y_c near $\pi/2$ but not ω or λ.

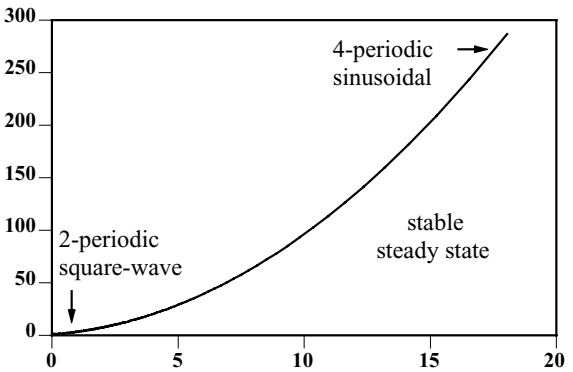

Fig. 4. First Hopf bifurcation of Ikeda equation. The Hopf bifurcation moves to infinity as the delay becomes small (ε becomes large). For small ε, the Hopf bifurcation quickly leads to two-periodic square-wave oscillations as λ increases while the oscillations remain nearly sinusoidal and are four-periodic for large ε.

3. Periodic solutions

We consider the $f_y < 0$ Hopf bifurcation and assume that the basic steady state is stable (all the σ_r are negative except one which is zero). In order to investigate the change of stability of the steady state, we need to determine σ_r for λ close to λ_c. We first expand $y_s - y_c$ for $\lambda - \lambda_c$ small and then seek a solution of Eqs. (17) and (18) in power series of $\lambda - \lambda_c$. This leads to $\sigma_r \simeq (\lambda - \lambda_c)\alpha$, where α has a complicated expression. The analysis of the sign of α is however simple. We find that $\sigma_r > 0$ ($\sigma_r > 0$) if $\lambda > \lambda_c$ provided that

$$a(\varepsilon) \equiv 2f_y \left(f_{yy} \frac{f_\lambda}{1 - f_y} + f_{y\lambda} \right) > 0 \ \ (< 0). \tag{32}$$

This function $a(\varepsilon)$ will reappear in our analysis. We next apply the Lindstedt–Poincaré method [7,36] and seek a 2π-periodic solution of the form

$$y = y_s + \delta y_1(s) + \delta^2 y_2(s) + \delta^3 y_3(s) + \cdots, \tag{33}$$

where y_i ($i = 1, 2, \ldots$) are 2π-periodic functions of s. Time s and the parameter δ are defined by

$$s \equiv (\omega_0 + \delta^2 \omega_2 + \cdots)t, \tag{34}$$

$$\lambda - \lambda_c \equiv \delta^2 c \quad (c = 1 \text{ or } -1). \tag{35}$$

The perturbation analysis is standard and we summarize the main result. Note, however, that we need to take account the expansion of the delayed variable, i. e.,

$$y(t-1) = y(s - \omega_0) - \delta^2 \omega_2 y'(s - \omega_0) + \cdots. \tag{36}$$

The leading approximation of the solution is

$$y \simeq y_c + \delta(A \exp(\mathrm{i}s) + \text{c.c.}) + \mathrm{O}(\delta^2), \tag{37}$$

where c. c. means complex conjugate and the complex amplitude A satisfies a solvability condition. If $|A| \neq 0$, the real and imaginary parts lead to two equations for the unknowns ω_2 and $|A|^2$. One of these equations provides a relatively simple expression for the correction of the frequency given by

$$\omega_2 = \frac{A\bar{A} f_{yy}^2 f_y}{f_y^2 + 1} \frac{\varepsilon^3 \omega^3}{D}, \tag{38}$$

where f_y and f_{yy} represent partial derivatives of the function f evaluated at $(\lambda, y) = (\lambda_c, y_c)$. D is defined by

$$D \equiv (f_y - 1 + \varepsilon^2\omega^2)^2 + 4\varepsilon^2\omega^2(f_y - 1)^2. \tag{39}$$

Since we consider the $f_y < 0$ Hopf bifurcation, we conclude from (38) that the sign of ω_2 is always negative whatever $f(\lambda, y)$ meaning that the period of the oscillations always increase as the amplitude of the solution increases.

Using (38), we eliminate ω_2 in the remaining solvability condition and obtain an equation for $|A|^2$ of the form

$$A\bar{A}F + a(2f_y)^{-1}c = 0, \tag{40}$$

where a is defined in (32) and

$$F \equiv f_{yy}^2 \left(\frac{1}{1 - f_y} + \frac{1}{2f_y D(f_y^2 + \varepsilon)} [(f_y^2 + \varepsilon)((f_y - 1)(1 + 3\varepsilon^2\omega^2) + (1 - \varepsilon^2\omega^2)\varepsilon^2\omega^2) - \varepsilon^5\omega^4 2f_y] \right) + \frac{f_{yyy}}{2}. \tag{41}$$

The inequality $A\bar{A} > 0$ then determines the sign of c, or equivalently from (35), the sign of $\lambda - \lambda_c$.

3.1. Ikeda small delay

In the limit of small delays ($\varepsilon \to \infty$), we find from (38) and (40)

$$\omega_2 = -\varepsilon^{-2}\frac{4}{11\pi - 4}, \tag{42}$$

$$|A|^2 = \varepsilon^{-4}\frac{80}{11\pi - 4}. \tag{43}$$

We have verified that these results correctly match the small amplitude limit of the ε large approximation of the original nonlinear problem [10]. From (33), we conclude that the leading order solution has the form

$$y = \frac{\pi}{2} - 2\varepsilon^{-1} + 2\delta\varepsilon^{-2}\sqrt{\frac{80}{11\pi - 4}}\,\sin(s) + \mathrm{O}(\delta^2). \tag{44}$$

From the second and third term in (44), we note that this expansion becomes nonuniform as soon as δ approaches $\mathrm{O}(\varepsilon)$ large quantities. This suggests that the perturbation solution remains valid even for large δ meaning that the oscillations remain nearly sinusoidal for small delay.

3.2. Large delay for an arbitrary function $f(\lambda, y)$

In the large delay limit ($\varepsilon \to 0$) using the fact that $f_y = -1$,we find that

$$\omega_2 = -\tfrac{1}{4} f_{yy}^2 \varepsilon^3 \pi^3, \tag{45}$$

$$|A|^2 = -\frac{a_0 c}{3b} > 0, \tag{46}$$

where the coefficients a_0 and b are defined as

$$a_0 = a(0) \equiv -2\left(f_{yy}\frac{f_\lambda}{2} + f_{y\lambda}\right) \quad \text{and} \quad b \equiv -\left(\frac{1}{2}f_{yy}^2 + \frac{f_{yyy}}{3}\right). \tag{47}$$

From (45), we learn that ω_2 is $\mathrm{O}(\varepsilon^3)$ small meaning, using (27) and (34), that the frequency of the oscillations remain close to π (period $P = 2$). Using (46), the leading expression of the solution for small ε has the form

$$\begin{aligned} y = y_s &+ \delta(A\exp(\mathrm{i}s) + \mathrm{c.c.}) + \frac{\delta^2}{4} f_{yy}[2A\bar{A} + A^2\exp(2\mathrm{i}s) + \mathrm{c.c.}] \\ &- \delta^3\left[\frac{A^3}{3i\varepsilon\pi}\left(\frac{3}{4}f_{yy} + \frac{1}{6}f_{yyy}\right)\exp(3\mathrm{i}s) + \mathrm{c.c.}\right] + \mathrm{O}(\delta^4). \end{aligned} \tag{48}$$

Note the $\mathrm{O}(\varepsilon^{-1})$ large term appearing in the $\mathrm{O}(\delta^3)$ contribution. The expansion (48) becomes nonuniform as soon as the $\mathrm{O}(\delta^3)$ and $\mathrm{O}(\delta^2)$ corrections are comparable, i. e., as

$$\delta = \mathrm{O}(\varepsilon). \tag{49}$$

Using (35), the scaling (49) suggest that the perturbation solution is no more valid as soon as $\lambda - \lambda_c = \mathrm{O}(\varepsilon^2)$. The amplitude of the Hopf bifurcation solution is well described in (46) if $\delta \ll \varepsilon$. But if δ comes closer to ε, the oscillations are no more harmonic and become more and more square-wave (see Fig. 5). Practically, we need to review the bifurcation problem as a singular perturbation problem where the amplitude of the solution and the deviation of the bifurcation point from its critical value are both scaled with respect to ε [2].

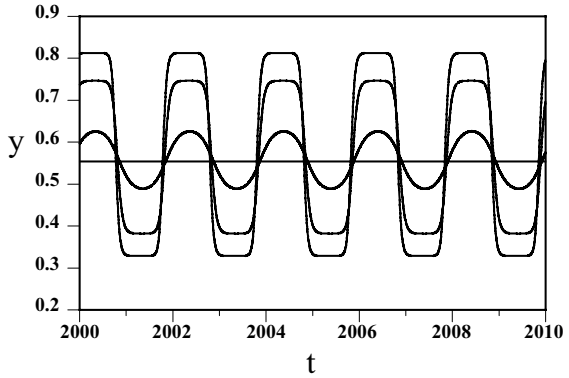

Fig. 5. Periodic solutions of Ikeda DDE near the first Hopf bifurcation point. $\varepsilon = 10^{-2}$ and $\lambda = 1.17, 1.18, 1.19, 1.20$. Since $\lambda_0 = 1.177$, the first value of λ corresponds to a stable steady state and the three next values correspond to the deviations $\lambda - \lambda_0 = 3 \times 10^{-3}$, 13×10^{-3} and 23×10^{-3}, respectively.

3.3. Ikeda large delay

In the case of Ikeda function (12), we may evaluate the partial derivatives. We find

$$f_{yy} = \lambda_0 - y_0, \qquad f_\lambda = \frac{y_0}{\lambda_0}, \qquad f_{y\lambda} = -\frac{1}{\lambda_0}, \qquad f_{yyy} = 1. \tag{50}$$

Using the Hopf conditions (21) and (28), it is possible to rewrite a_0 as

$$a_0 = \frac{1}{\lambda_0}(1 + \lambda_0 y_0), \tag{51}$$

which is always positive. We also note from (47) and the fact that $f_{yyy} > 0$ that b is always negative. From (46), we then conclude that c is always positive implying a supercritical bifurcation.

4. Singular Hopf bifurcation

In the previous section, we showed that the regular expansion of the Hopf bifurcation solution fails to gives the correct description as soon as (49) is verified. In this case, we need to reexamine the asymptotic problem by a more detailed analysis where the two small parameters, namely $\lambda - \lambda_0$ and ε are related. The need for such an analysis was anticipated in [4] where $O(\varepsilon)$ transition layers between plateaus of square-wave solutions are constructed. In the special case $f(\lambda, y) = -(1 + \lambda)y + ay^2 + by^3 + \cdots$ as $y \to 0$, center manifold techniques have been used for small λ and ε in order to determine the periodic solutions from sine to square-waves. See [5,19] for the supercritical and subcritical cases, respectively. Here, we prefer to use a modified Lindstedt–Poincaré method which allows us to handle the general function $f(\lambda, y)$ without pre-treatment of the original equation. We also verify that our solution correctly matches the Hopf bifurcation solution as $\lambda - \lambda_0 \to 0$ and the solution determined from the map as $\lambda - \lambda_0 \gg \varepsilon^2$. Finally, we compare analytical and numerical bifurcation diagrams in the case of Ikeda nonlinearity.

We concentrate on the first Hopf bifurcation. A detailed analysis that considers all the (stable or unstable) Hopf bifurcations and the effect of modulation is given in [39]. The scaling (49) suggests to replace the expansion (33) by an expansion in power series of ε. Similarly, (35) and the fact that

$$\lambda_c(\varepsilon) = \lambda_0 + \varepsilon^2 \lambda_1 + \cdots, \tag{52}$$

where

$$\lambda_1 \equiv \frac{\pi^2}{a_0}, \tag{53}$$

suggests that the first term in the expansion $\lambda - \lambda_0$ should be in ε^2. We also note from (22) that

$$\omega(\varepsilon) = \pi - \varepsilon\pi + \varepsilon^2\pi + \cdots, \tag{54}$$

suggesting that we need to look for corrections of the frequency in power series of ε. Specifically, we seek a two-periodic solution of the form

$$y = y_0 + \varepsilon y_1(S) + \varepsilon^2 y_2(S) + \cdots, \tag{55}$$

$$\lambda = \lambda_0 + \varepsilon^2 \Lambda + \varepsilon^3 \Lambda_1 + \cdots, \tag{56}$$

where S is now defined as

$$S \equiv (1 + \varepsilon\Omega_1 + \varepsilon^2\Omega_2 + \cdots)t. \tag{57}$$

The perturbation analysis is no more a routine application of the method and we give some details. First, we need to rewrite the delayed variable in terms of S. Using (57), we find

$$y(t-1) = y(S-1) - (\varepsilon\Omega_1 + \varepsilon^2\Omega_2 + \cdots)y'(S-1) + \frac{\varepsilon^2\Omega_1^2}{2}y''(S-1) + \cdots. \tag{58}$$

Introducing (55)–(58) into (8), we equate to zero the coefficients of each power of ε. The first three problems are given by

$$\mathrm{O}(\varepsilon) : Ly_1 \equiv y_1 + y_1(S-1) = 0, \tag{59}$$

$$\mathrm{O}(\varepsilon^2) : Ly_2 = \tfrac{1}{2}f_{yy}y_1^2(S-1) + f_\lambda\Lambda + \Omega_1 y_1'(S-1) - y_1', \tag{60}$$

$$\begin{aligned}\mathrm{O}(\varepsilon^3) : Ly_3 = {} & f_{yy}y_1(S-1)y_2(S-1) + \tfrac{1}{6}(f_{yyy})y_1^3(S-1) - \Omega_1 y_1' - y_2' + \Omega_2 y_1'(S-1) + \Omega_1 y_2'(S-1) \\ & - \tfrac{1}{2}\Omega_1^2 y_1''(S-1) - f_{yy}\Omega_1 y_1(S-1)y_{1S}(S-1) + f_{y\lambda}\Lambda y_1(S-1) + f_y\Lambda_1,\end{aligned} \tag{61}$$

where all partial derivatives are evaluated at $(\lambda, y) = (\lambda_0, y_0)$. Eq. (59) implies that y_1 is an odd periodic function of S satisfying the condition

$$y_1(S-1) = -y_1(S). \tag{62}$$

The left hand side of Eq. (60) admits an odd periodic solution. Solvability then requires that

$$\Omega_1 y_1'(S-1) - y_1' = (\Omega_1 + 1)y_1' = 0, \tag{63}$$

which implies

$$\Omega_1 = -1. \tag{64}$$

The solution of Eq. (60) is then of the form

$$y_2 = y_{20}(S) + \tfrac{1}{2}[\tfrac{1}{2}f_{yy}y_1^2 + f_\lambda\Lambda], \tag{65}$$

where y_{20} is a new unknown odd function of S satisfying

$$y_2(S-1) = -y_2(S). \tag{66}$$

Next, we consider Eq. (61) and apply a solvability condition with respect to all odd periodic functions. After simplifying, we obtain

$$-(\tfrac{1}{4}f_{yy}^2+\tfrac{1}{6}f_{yyy})y_1^3-(\tfrac{1}{2}f_\lambda f_{yy}+f_{y\lambda})\Lambda y_1+y_1'(1-\Omega_2)+\tfrac{1}{2}y_1''=0. \tag{67}$$

Analyzing the solution of this equation in the phase plane (y, y') shows that a periodic orbit is only possible if the coefficient of y_1' is zero. We thus requires that

$$\Omega_2=1, \tag{68}$$

and Eq. (67) reduces to

$$y_1''+a_0\Lambda y_1+by_1^3=0, \tag{69}$$

where a_0 and b are the coefficients defined in (47). This equation is analyzed in Appendix A for the case $a_0\Lambda>0$ and $b<0$ as it is verified for the Ikeda function. We obtain a parametric solution for $y_{\max}(\Lambda)$ given by

$$y_{\max}-y_0=\varepsilon\sqrt{\frac{-2\nu}{b}}2K(\nu), \tag{70}$$

$$\Lambda=\frac{1}{a_0}(1+\nu)4K^2(\nu), \tag{71}$$

where $0\le\nu<1$ and $K(\nu)$ is defined as the complete elliptic function of the first kind [1] (see (A. 15)). As $\nu\to 0$, we have $K=(\pi/2)(1+(1/4)\nu+\cdots)$, $\Lambda=(\pi^2/a)(1+3\nu/2+\cdots)$, and

$$y_{\max}-y_0\simeq 2\varepsilon\sqrt{-\frac{a_0(\Lambda-\lambda_1)}{3b}}. \tag{72}$$

This result is matching the $\varepsilon=0$ limit of our small δ small expansion. This can be verified as follows. Using (46) and the fact that $y_{\max}-y_c\simeq 2\delta|A|$, we find

$$y_{\max}-y_0=2\delta\sqrt{-\frac{a_0c}{3b}}. \tag{73}$$

We note that $\delta^2c=(\lambda-\lambda_c)=(\lambda-\lambda_0-\varepsilon^2\lambda_1)=\varepsilon^2(\Lambda-\lambda_1)$ and (72) and (73) are identical in first approximation. On the other hand, as $\nu\to 1$, $\Lambda\to\infty$ and

$$y_{\max}-y_0\simeq\varepsilon\sqrt{\frac{-a_0\Lambda}{b}}. \tag{74}$$

This expression is matching a branch of square-wave solutions described by a map, as we shall now show. As λ progressively deviates from the Hopf bifurcation point (i. e., as soon as $\lambda-\lambda_c=\mathrm{O}(\varepsilon^2)$), the bifurcating and stable periodic solution changes from harmonic to square-wave oscillations (see Fig. 5). We may capture the plateaus of these square-wave oscillations by analyzing the equation for the map given in (10). Fixed points of Eq. (10) correspond to the plateaus of the square-wave oscillations. The bifurcation diagram of the solutions of Ikeda map has been investigated in detail (see, for example [34]). Note that the periodic solution is a square-wave pattern with half-period close to 1 and with sharp $\mathrm{O}(\varepsilon)$ small transition layers. Equations for these transition layers can be formulated but are difficult to solve [4]. However, we may analyze the Hopf bifurcation of Eq. (10). A limit-cycle solution corresponds to a P2 fixed point of Eq. (10) satisfying the conditions

$$y_{n+1}=f(\lambda, y_n), \tag{75}$$

$$y_n=f(\lambda, y_{n+1}). \tag{76}$$

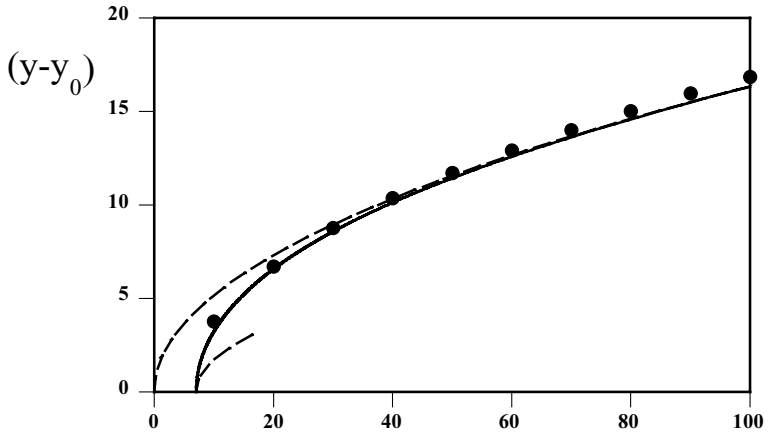

Fig. 6. Singular Hopf bifurcation. The singular perturbation analysis assuming $\lambda - \lambda_0 = O(\varepsilon^2)$ and $y - y_0 = O(\varepsilon)$ describes how the solution progressive changes from harmonic to square-wave oscillations (full line in the figure). The broken line emerging from $\lambda - \lambda_0 = \varepsilon^2 \lambda_1$ corresponds to the regular Hopf bifurcation approximation. The broken line emerging from $\lambda - \lambda_0 = 0$ is the approximation coming from the equation for the map. Dots represent values obtained numerically by integrating the Ikeda DDE.

We may solve these equations for (y, λ) close to the Hopf bifurcation point (y_0, λ_0). We find that the deviation $u_n = y_n - y_0$ satisfies the bifurcation equation

$$0 = a_0 \Lambda u_n + b u_n^3, \tag{77}$$

where a_0 and b are defined in (47). Eq. (77) then gives

$$u_n = \sqrt{-\frac{a_0 \Lambda}{b}}, \tag{78}$$

which is correctly matching (74). See Fig. 6 for a comparison between numerical and analytical solutions.

5. Summary

In this paper, we reexamined the Hopf bifurcation for a class of DDEs that includes Ikeda original equation both for small and large delays. We find that stable and unstable Hopf bifurcation points are possible and investigate the first stable Hopf bifurcation in detail. For small delays, we show that a Hopf bifurcation remains possible provided the feedback rate is strong enough (Hopf bifurcation from infinity). For large delays, we complement the early work by Chow et al. [5] and Hale and Huang [19] by comparing analytical and numerical bifurcation diagrams as the oscillations progressively change from sine to square-wave. Our analysis is done in the spirit of the theory of matched asymptotic expansions and we have verified that matching between three distinct solutions. The direction of bifurcation is also reevaluated analytically in terms of an arbitrary control parameter distinct from the delay. Our results indicate that the period of the oscillations always increases as the amplitude of the oscillations increases whatever the form of the function $f(\lambda, y)$. The bifurcation can be either supercritical or subcritical but the latter case is not possible for the Ikeda function because the nonlinearity is sinusoidal. The observation of a subcritical bifurcation needs different nonlinearities and this bifurcation is analyzed numerically and experimentally in [30]. The analysis given in terms of an arbitrary function $f(\lambda, y)$ could be extended to hybrid systems (differential difference equations coupled with difference equations) or scalar DDEs with several delays [20].

Acknowledgements

The research was supported by the European Office of Aerospace Research and Development, Air Force Office of Scientific Research, under contract F61775-01-WE036, the National Science Foundation grant DMS-9973203, the Fonds National de la Recherche Scientifique (Belgium) and the InterUniversity Attraction Pole program of the Belgian government.

Appendix A

In this appendix, we seek a two-periodic solution of the following equation:

$$\frac{\mathrm{d}^2 y}{\mathrm{d}S^2} + ay + by^3 = 0, \tag{A. 1}$$

that satisfies the condition

$$y(S) = -y(S-1). \tag{A. 2}$$

Condition (A. 2) means that the solution must be an odd function of s. A first integration of Eq. (A. 1) gives

$$\frac{1}{2}\left(\frac{\mathrm{d}y}{\mathrm{d}S}\right)^2 + a\frac{y^2}{2} + b\frac{y^4}{4} = E, \tag{A. 3}$$

where E is the constant of integration. The maximum and minimum of y satisfy the quadratic equation

$$y^4 + 2\left(\frac{a}{b}\right)y^2 - \frac{4E}{b} = 0. \tag{A. 4}$$

We consider the case

$$a > 0, \quad b < 0 \ \text{ and } \ 0 < E < -\frac{a^2}{4b}. \tag{A. 5}$$

Then

$$y_{\max} = \sqrt{-\frac{a}{b} - \sqrt{\left(\frac{a}{b}\right)^2 + \frac{4E}{b}}} = -y_{\min}, \tag{A. 6}$$

and

$$S = \int_{y_{\min}}^{y} \frac{\mathrm{d}v}{\sqrt{2[E - (a/2)v^2 - (b/4)v^4]}} \quad \left(\frac{\mathrm{d}y}{\mathrm{d}S} > 0\right), \tag{A. 7}$$

$$S = -\int_{y_{\max}}^{y} \frac{\mathrm{d}v}{\sqrt{2[E - (a/2)v^2 - (b/4)v^4]}} \quad \left(\frac{\mathrm{d}y}{\mathrm{d}S} < 0\right). \tag{A. 8}$$

Introducing the new parameters

$$\nu \equiv -\frac{by_{\max}^4}{4E}, \tag{A. 9}$$

$$\xi \equiv \frac{v}{y_{\max}}, \tag{A. 10}$$

we find

$$\frac{ay_{\max}^2}{2E} = 1 + \nu, \tag{A. 11}$$

and (A. 7), (A. 8) simplify as

$$S = \frac{y_{\max}}{\sqrt{2E}} \int_{-1}^{y/y_{\max}} \frac{\mathrm{d}\xi}{\sqrt{2(1-\xi^2)(1-\nu\xi^2)}}, \tag{A. 12}$$

$$S = -\frac{y_{\max}}{\sqrt{2E}} \int_{1}^{y/y_{\max}} \frac{\mathrm{d}\xi}{\sqrt{2(1-\xi^2)(1-\nu\xi^2)}}. \tag{A. 13}$$

We consider the simplest solution of period which satisfies the condition

$$2 = \frac{y_{\max}}{\sqrt{2E}} \int_{-1}^{1} \frac{\mathrm{d}\xi}{\sqrt{(1-\xi^2)(1-\nu\xi^2)}} = \frac{y_{\max}}{\sqrt{2E}} \times 2K(\nu), \tag{A. 14}$$

where

$$K(\nu) \equiv \int_0^1 \frac{\mathrm{d}\xi}{\sqrt{(1-\xi^2)(1-\nu\xi^2)}} \tag{A. 15}$$

is defined as the complete elliptic integral of the first kind [1]. From (A. 14), we eliminate E and obtain $y_{\max}$ as

$$y_{\max} = \sqrt{\frac{-2\nu}{b}} 2K(\nu). \tag{A. 16}$$

Then using (A. 11), we obtain

$$a = (1+\nu)4K^2(\nu). \tag{A. 17}$$

References

[1] M. Abramowitz, I. Stegun (Eds.), Handbook of Mathematical Functions, 9th ed., Dover, New York, 1972.

[2] S. M. Baer, T. Erneux, Singular Hopf bifurcation to relaxation oscillations, SIAM J. Appl. Math. 46 (1986) 721–739;
S. M. Baer, T. Erneux, Singular Hopf bifurcation to relaxation oscillations II, SIAM J. Appl. Math. 52 (1992) 1651–1664.

[3] C. M. Bender, S. A. Orszag, Advanced Mathematical Methods for Scientists and Engineers, McGraw-Hill, New York, 1978.

[4] S.-N. Chow, J. Mallet-Paret, Singularly perturbed delay-differential equations, in: J. Chandra, A. C. Scott (Eds.), Coupled Nonlinear Oscillators, North-Holland, Amsterdam, 1983, pp. 7–12.

[5] S. N. Chow, J. K. Hale, W. Huang, From sine waves to square-waves in delay equations, Proc. Roy. Soc. Edinburgh A 120 (1992) 223–229.

[6] O. Diekmann, S. A. van Gils, S. M. Verduyn Lunel, H.-O. Walther, Delay Equations, Springer, New York, 1995.

[7] P. G. Drazin, Nonlinear Systems, Cambridge Texts in Applied Mathematics, Cambridge University Press, Cambridge, 1992.

[8] R. D. Driver, Ordinary and Delay Differential Equations, Applied Mathematical Sciences, vol. 20, Springer-Verlag, New York, 1977.

[9] J. Duvernoy, J.-P. Goedgebuer, H. Porte, Bistabilité, multistabilité et chaos en longueur d'onde, Ann. Télécomun. 42 (1987) 315–323.

[10] T. Erneux, L. Larger, K. Green, D. Roose, Modelling nonlinear optics phenomena using delay differential equations, Proc. Equadiff., in press.

[11] A. C. Fowler, Mathematical Models in the Applied Sciences, Cambridge Texts in Applied Mathematics, Cambridge University Press, Cambridge, 1997.

[12] A. Fowler, An asymptotic analysis of the delayed logistic equation when the delay is large, IMA J. Appl. Math. 28 (1982) 41–49.

[13] F. Giannakopoulos, A. Zapp, Local and global Hopf bifurcation in scalar delay differential equation, J. Math. Anal. Appl. 237 (1999) 425–450.

[14] F. Giannakopoulos, A. Zapp, Stability and Hopf bifurcation in differential equations with one delay, Nonlinear Dyn. Syst. Theor. 1 (2001) 23–36.

[15] H. M. Gibbs, F. A. Hopf, D. L. Kaplan, R. Shoemaker, Observation of chaos in optical bistability, Phys. Rev. Lett. 46 (1981) 474–477.

[16] J.-P. Goedgebuer, M. Li, H. Porte, Demonstration of bistability and multistability in wavelength with a hybrid acousto-optic device, IEEE J. Quant. Electron. 23 (1987) 153–157.

[17] J.-P. Goedgebuer, L. Larger, H. Porte, F. Delorme, Chaos in wavelength with feedback tunable laser diode, Phys. Rev. E 57 (1998) 2795–2798.

[18] J. Guckenheimer, P. H. Holmes, Nonlinear Oscillators, Dynamical Systems and Bifurcation of Vector Fields, Springer-Verlag, New York, 1986.

[19] J. K. Hale, W. Huang, Period doubling in singularly perturbed delay equations, J. Diff. Equ. 114 (1994) 1–23.
[20] J. K. Hale, Effects of delays on dynamics, in: A. Granas, M. Frigon, G. Sabidussi (Eds.), Topological Methods in Differential Equations and Inclusions, Kluwer Academic Publishers, Dordrecht, 1995.
[21] Z. Hong, Z. Feizhou, Y. Jie, W. Yinghai, Nonlinear differential delay equations using the Poincaré section technique, Phys. Rev. E 54 (1996) 6925–6928.
[22] F. A. Hopf, D. L. Kaplan, H. M. Gibbs, R. L. Shoemaker, Bifurcation to chaos in optical bistability, Phys. Rev. A 25 (1982) 2172–2182.
[23] K. Ikeda, Multiple-valued stationary state and its instability of the transmitted light by a ring cavity system, Opt. Comm. 30 (1979) 257–261.
[24] K. Ikeda, H. Daido, O. Akimoto, Optical turbulence: chaotic behavior of transmitted light from a ring cavity, Phys. Rev. Lett. 45 (1980) 709–712.
[25] K. Ikeda, O. Akimoto, Instability leading to periodic and chaotic self-pulsations in a bistable optical cavity, Phys. Rev. Lett. 48 (1982) 617–620.
[26] G. Ioos, D. D. Joseph, Elementary Stability and Bifurcation Theory, 2nd ed., Springer, Berlin, 1991.
[27] J. Kevorkian, J. D. Cole, Perturbation Methods in Applied Mathematics, Applied Mathematical Sciences, vol. 34, Springer, New York, 1981;
J. Kevorkian, J. D. Cole, Multiple Scale and Singular Perturbation Methods, Applied Mathematical Sciences, vol. 114, Springer, New York, 1996.
[28] L. Larger, J.-P. Goedgebuer, J.-M. Merolla, Chaotic oscillator in wavelength: a new setup for investigating differential difference equations describing nonlinear dynamics, IEEE J. Quant. Electron. 34 (1998) 594–601.
[29] L. Larger, M. W. Lee, J.-P. Goedgebuer, W. Elflein, T. Erneux, Chaos in coherence modulation: bifurcations of an oscillator generating optical delay fluctuations, JOSA B 18 (2001) 1063–1068.
[30] L. Larger, J.-P. Goedgebuer, T. Erneux, Subcritical Hopf bifurcation in dynamical systems described by a scalar nonlinear delay differential equation, Phys. Rev. E, in press.
[31] M. W. Lee, Etude des comportements chaotiques en modulation de cohérence et application à la crytographie, Ph. D. Thesis, UFR des Sciences et techniques de l'Université de Franche-Comté, 2002.
[32] M. C. Mackey, Mathematical models of hematopoietic cell replication and control, in: H. Othmer, F. Adler, J. Dallon, M. Lewis (Eds.), Case Studies in Mathematical Modeling: Ecology, Physiology and Cell Biology, Prentice-Hall, Upper Saddle River, NJ, 1996, pp. 149–178.
[33] P. Mandel, Theoretical Problems in Cavity Nonlinear Optics, Cambridge Studies in Modern Optics, Cambridge University Press, Cambridge, 1997.
[34] P. Mandel, R. Kapral, Subharmonic and chaotic bifurcation structure in optical bistability, Opt. Comm. 47 (1983) 151–156.
[35] P. Nardone, P. Mandel, R. Kapral, Analysis of a delay-differential equation in optical bistability, Phys. Rev. A 33 (1986) 2465–2471.
[36] A. Nayfeh, Perturbation Methods, Wiley/Interscience, New York, 1973.
[37] A. C. Newell, J. V. Moloney, Nonlinear Optics, Addison-Wesley, New York, 1992.
[38] A. Neyer, E. Voges, Dynamics of electrooptic bistable devices with delayed feedback, IEEE J. Quantum. Electron. 18 (1982) 2009–2015.
[39] M. Nizette, Front dynamics in a delayed-feedback system with external forcing, Physica D 183 (2003) 220–244.
[40] K. Otsuka, Nonlinear Dynamics in Optical Complex Systems, KTK Scientific Publishers/Kluwer Academic Publishers, Tokyo/Boston, 1999.
[41] S. Rosenblat, S. H. Davis, Bifurcation from infinity, SIAM J. Appl. Math. 37 (1979) 1–19.
[42] M. Schanz, A. Pelster, Analytical and numerical investigations of the phase-locked loop with time delay, Phys. Rev. E 67 (2003) 056205.
[43] R. Vallée, C. Delisle, Mode description of the dynamical evolution of an acousto-optic bistable device, IEEE J. Quant. Electron. 21 (1985) 1423–1428.